Electrical Conductance of Cryptate Solutions: Comparison between Experiments and Simulation Results

M. Jardat, O. Bernard, C. Treiner, and P. Turq*

Laboratoire Liquides Ioniques et Interfaces Chargées, boîte postale 51, Université P. et M. Curie, 4 place Jussieu, F-75252 Paris Cedex 05, France

Received: April 26, 1999; In Final Form: June 29, 1999

Smart Brownian dynamics have been used to compute the electrical conductance of aqueous cryptate chloride solutions; the results are compared to experimental data. The numerical simulations take into account both direct and hydrodynamic interactions between ions. Direct interactions are modelled by pairwise soft-core interactions and several interaction potentials are compared; hydrodynamic interactions are evaluated by a modified Rotne-Prager tensor, which can be used even if two particles overlap. It is shown that the experimental data can be interpreted by numerical simulations if the interaction potential between ions contains a short-range attractive contribution in addition to the Coulomb and the short-range repulsive parts.

1. Introduction

Some alkali and alkaline-earth metal cations can form stable inclusion complexes with cryptand molecules[1] in solution, which are called cryptate ions. The stability constants of such complexes have been determined from different experimental techniques (see, e.g., refs 2−4). In particular, a potassium ion can be trapped in the cavity of the cryptand 4,7,13,16,21,24-hexaoxa-1,10-diazabicyclo-8.8.8-exacosane[2.2.2] (referred to by the abbreviation 222 throughout the text), to form a strong complex in aqueous solution.

The structure of aqueous and nonaqueous solutions of several cryptates has been studied in this laboratory by small-angle neutron scattering (SANS) experiments.[5,6] The hypernetted chain (HNC) integral equation with solvent-averaged pair potentials was used to describe the scattering spectra; it was shown that, despite their similar charges, cryptated potassium ions can come into close contact. The effective pair interaction potential fitted from these SANS experiments contains indeed a short-range attractive contribution between the pairs cryptate−cryptate and cryptate−chloride in addition to the Coulomb and the short-range repulsive potentials.

In the present paper, we study the dynamical properties of cryptate solutions, which can provide additional informations concerning these systems; in particular, the computation and the measurement of the electrical conductance, which is usually decreased when ions of opposite charges are associated, can give further indications about the interactions between ions.

The purpose of this work is to use numerical simulations in order to calculate the electrical conductance of aqueous $222K^+,Cl^-$ solutions. In particular, we propose to investigate whether the interaction potential proposed by Cartailler et al.[6] to recover the experimental SANS spectrum of this solution at 0.5 mol/L allows the conductance to be computed in agreement with experimental data. As the cryptates are heavy ions, roughly of spherical shape, they are convenient models for Brownian particles; their structural and dynamical properties in solution can then be studied by simulations based on a continuous solvent model, such as the Brownian dynamics method. Recently, we have proposed an efficient Brownian dynamics (BD) simulation method, called smart BD, which uses a smart Monte Carlo algorithm[7] and includes a description of hydrodynamic interactions (HI);[8] it allows the computation of transport coefficients of aqueous solutions in the molar concentration range. It has been shown in the case of aqueous KCl solutions[8] and aqueous NaCl/KCl mixtures[9] that a correct description of the self-diffusion coefficients and of the conductance requires the introduction of HI. We propose here to compute the conductance of K^+222,Cl^- aqueous solutions from BD simulations including HI. The results obtained by using the interaction potential proposed by Cartailler et al. are compared to experimental data, and this interaction potential is modified in order to obtain agreement with the experiments. Hydrodynamic interactions are evaluated by a modified Rotne−Prager[10] tensor, as the short-range attractive contribution to the interaction potential can yield an overlap between ions.

The paper is organized as follows. In section 2 we describe the experimental conditions of the conductance measurements and the results obtained. The simulation procedure is presented in section 3. The results of simulations are compared to our experiments in section 4.

2. Experimental Section

The cryptand 222 was from Merck (Kryptofix for synthesis), and potassium chloride was a Normapur compound (Rhône-Poulenc). Water was purified by ion exchange, microfiltration, and photooxidation (Elgastat Maxima). The solutions were made up by weight. The density of the solutions were measured at 25.0 ± 0.1 °C using a densimeter from Paar (model DMA 38). The variation of the density of the cryptand solution in the presence of a constant KCl concentration was found linear in the domain investigated, i.e., $c < 0.15$ mol/L: $d = 1.0012 + 0.048\,c$, where c is the molar concentration of the cryptand.

The conductivity cell (Inforlab Chimie) has platinized electrodes. The cell constant was determined using the method of Lind, Zwolenik and Fuoss[11,12] using aqueous KCl solutions in a concentration domain below 0.01 mol/L. The constant was found equal to 0.9521 ± 0.0008 cm^{-1}. The cell was immersed in a water bath the temperature being maintained constant at

* Corresponding author. E-mail: pt@ccr.jussieu.fr.

10.1021/jp991350e CCC: $18.00
Published on Web 09/15/1999

TABLE 1: Experimental Equivalent Conductance of 222K$^+$,Cl$^-$ Aqueous Solutions at 298 K

first series of measurements			second series of measurements		
c [mol/L]			c [mol/L]		
222	KCl	Λ [cm^2/Ω/mol]	222	KCl	Λ [cm^2/Ω/mol]
0	0.1001	128.82	0	0.1508	126.52
0.1049	0.1006	71.5	0.1464	0.1519	65.9
0.0874	0.0837	74.6	0.1548	0.1519	63.7
0.0749	0.0717	76.5	0.1290	0.1264	66.9
0.0617	0.0590	79.0	0.1106	0.1083	69.5
0.0524	0.0502	81.0	0.0967	0.0947	71.6
0.0420	0.0401	83.5	0.1505	0.0947	71.2
0.0350	0.0334	84.8			

25.0 ± 0.01 °C. The solution resistances were measured with a Wayne-Kerr bridge (model 6425). The resistances were measured at four frequencies: 10, 5, 2, and 1 kHz, and extrapolated to infinite frequency in the usual way. The slopes of the lines were identical at all cryptate concentrations but were somewhat higher than the corresponding slope for pure KCl solutions.

The following experimental procedure was employed: the conductance of pure water was first measured, then the solid KCl crystals were added. This enables to check the purity of the solution. Then the solid cryptand was added to the solution. Finally this solution was diluted at a constant ratio of cryptand to KCl concentrations by successive addition of known amounts of water. The solutions were homogenized with a magnetic stirrer after each addition.

Two series of measurements were performed. The first one had an initial KCl and cryptand concentrations of about 0.1 mol/L, the concentration of the latter compound being somewhat higher than for that of the former. The second run was made at initial concentrations of 0.15 mol/L. Table 1 presents the results of these two runs. The two series of measurements overlap within experimental uncertainty, which is on the order of 0.1%.

3. Simulation Method

3.1. Smart Brownian Dynamics Algorithm. On the mesoscopic time scale of Brownian dynamics, the motions are described in configuration space only. The numerical simulation is based on a stochastic equation of motion for the displacement $\Delta\mathbf{r}$ of the N particles from t to $t + \Delta t$:[13,14]

$$\Delta\mathbf{r} = \left(\beta\mathbf{D}\cdot\mathbf{F} + \frac{\partial}{\partial\mathbf{r}}\cdot\mathbf{D}\right)\Delta t + \mathbf{R} \tag{1}$$

where $\beta = 1/k_BT$. Here, the particles are supposed to be spherical, without rotational degrees of freedom; Δt is the time increment, $\mathbf{r} = (\mathbf{r}_1^T, \mathbf{r}_2^T, ..., \mathbf{r}_N^T)^T$ is the $3N$-dimensional configuration vector, and $\mathbf{F} = (\mathbf{F}_1^T, ..., \mathbf{F}_N^T)^T$ describes the forces acting on the particles at the beginning of the step. $\mathbf{R}$ is a random displacement, chosen from a Gaussian distribution with zero mean, $\langle\mathbf{R}\rangle = 0$, and variance $\langle\mathbf{R}\mathbf{R}^T\rangle = 2\mathbf{D}\Delta t$. Hydrodynamic interactions between particles are introduced via the configuration dependent $3N \times 3N$ diffusion tensor $\mathbf{D}$, whose evaluation will be presented in the next subsection. $\mathbf{D}$ becomes proportional to the unit matrix and constant when HI are neglected: $\mathbf{D} = D^0\mathbf{I}$.

The displacement $\Delta\mathbf{r}$ known from eq 1 is accepted with a criterion known from the smart Monte Carlo method.[7] The expression of the acceptance probability when HI are taken into account and a discussion concerning the so-called smart Brownian dynamics method are presented elsewhere.[8] The main interest of this method is the use of large time steps which allows one to attain simulation lengths largely exceeding the relaxation time of the Debye ionic atmosphere.

The specific conductance of the system can be computed from the simulations, by using the following Kubo-like expression:[8,15]

$$\chi_{sp} = \frac{1}{3}\frac{\beta}{V}\left(\left\langle\sum_{i=1}^{N}\sum_{j=1}^{N} q_i q_j\, tr\{\mathbf{D}_{ij}\}\right\rangle - \int_0^\infty dt\left\langle\sum_{i=1}^{N} q_i\mathbf{U}_i(0)\cdot\sum_{j=1}^{N} q_j\mathbf{U}_j(t)\right\rangle\right) \tag{2}$$

where q_i is the electrical charge of the ith particle and

$$\mathbf{U}_i = \sum_{j=1}^{N}\left[\beta\mathbf{D}_{ij}\cdot\mathbf{F}_j + \frac{\partial}{\partial\mathbf{r}_j}\cdot\mathbf{D}_{ij}\right] \tag{3}$$

is the hydrodynamic velocity of the ith particle.

3.2. Pair Interaction Potential. The effective interaction potential between ions has the following form:[16]

$$V_{ij}(r) = \frac{q_i q_j}{4\pi\epsilon_r\epsilon_0 r} + \mathrm{COR}_{ij}(r) + \mathrm{GUR}_{ij}(r) \tag{4}$$

Here the first term represents the Coulomb interaction between ions i and j: ϵ_0 is the permittivity of the vacuum and ϵ_r the relative permittivity of the pure solvent. Coulomb interactions are computed by using the Ewald summation technique.[17,18]

The second term describes a soft-core repulsive interaction potential:

$$\mathrm{COR}_{ij}(r) = \frac{1}{4\pi\epsilon_0}\frac{B_{ij}e^2}{(a_i + a_j)n_{ij}}\left(\frac{a_i + a_j}{r}\right)^{n_{ij}} \tag{5}$$

where a_i is the radius of the ith ion, e the elementary charge, and n_{ij} and B_{ij} are adjustable parameters.

The last term is the so-called Gurney potential,[16] which is a short-range attractive contribution: for $r < d_i + d_j$,

$$\mathrm{GUR}_{ij}(r) = \pi\frac{A_{ij}}{V_s}\left(-\frac{(d_i^2 - d_j^2)^2}{4r} + \frac{2}{3}(d_i^3 + d_j^3) - \frac{1}{2}r(d_i^2 + d_j^2) + \frac{r^3}{12}\right) \tag{6}$$

and for $r \geq d_i + d_j$

$$\mathrm{GUR}_{ij}(r) = 0 \tag{7}$$

where $d_i = a_i + s$ with s being the size of a solvent molecule, V_s is the molar volume of water ($V_s = 18.07$ cm^3/mol), and A_{ij} is an adjustable parameter, of negative sign in the cases studied here.

Three sets of parameters have been used to compute the conductance of 222K$^+$,Cl$^-$ aqueous solutions at 0.05, 0.1, and 0.15 mol/L. The first set of parameters is the one proposed by Cartailler et al.[6] to fit the HNC results to the SANS spectrum of an aqueous 222K$^+$,Cl$^-$ solution at 0.5 mol/L. It will be referred to by the abbreviation "GS potential" throughout the text. As it will appear in the following section, the results in this case are only in qualitative agreement with our experimental data. We have therefore chosen two other interaction potentials: (i) the first one contains only the first two terms of eq 4, i.e., only a short-range repulsive contribution in addition to the Coulomb forces. This potential will be referred to by the abbreviation "$1/r^{12}$ potential", as the repulsion is more intensive

TABLE 2: Parameters of the Effective Interaction Potentials

	GS			$1/r^{12}$			GC		
	++	+−	−−	++	+−	−−	++	+−	−−
B_{ij}	5×10^{-4}	4×10^{-4}	0.291	0.013	0.013	0.013	5×10^{-4}	4×10^{-4}	0.291
A_{ij} [J/mol]	−6	−40	0	0	0	0	−6	−100	0
n_{ij}	9	9	9	12	12	12	9	9	9

TABLE 3: Parameters of the Simulation at 298 K

c [mol/L]	L_{box} [Å]	Δt [ps]	τ_{Debye} [ps]	t_{total} [ps]	packing fraction
0.05	153.09	0.4	1433	32768	0.025
0.1	121.51	0.25	716	20480	0.05
0.15	106.15	0.2	478	16384	0.074

than in the GS one ($1/r^{12}$ instead of $1/r^9$), (ii) the second one is similar to the GS potential but contains a more intensive attractive contribution for the pair cryptate−chloride (-100 J/mol instead of −40 J/mol); it will be referred to by the abbreviation "GC potential" throughout the text.

In all cases, the radii of the particles are $a_{222K^+} = 5.75$ Å and $a_{Cl^-} = 1.81$ Å.[6] The parameters of the potentials are reported in Table 2; the abbreviations + and − are used for cryptate and chloride ions respectively. The coefficients B_{ij} of the $1/r^{12}$ potential, which determine the magnitude and extension of the repulsion, are all the same and have been chosen such that the minimum of the +− potential coincides with the distance $r = a_{222K^+} + a_{Cl^-}$.

In each simulation, 216 ions are placed in a cubic box with periodic boundary conditions; soft-core interactions are truncated outside half a box length, applying the minimum image convention. The temperature of the systems is 298 K. The conductance is computed by applying fast Fourier transform techniques[19] and is averaged over five successive trajectories, each containing 2^{16} time steps.

The time step Δt is chosen such that the acceptance ratio remains higher than 60%; in any case the length of the simulation (t_{total}) exceeds the Debye relaxation time (τ_{Debye}). The parameters of the simulations are presented in Table 3.

The self-diffusion coefficients at infinite dilution are taken from experiments: $D^0_{222K^+} = 0.55 \times 10^{-5}$ cm^2/s[20−22] and $D^0_{Cl^-} = 2.032 \times 10^{-5}$ cm^2/s.[23]

3.3. Hydrodynamic Diffusion Tensor. Hydrodynamic interactions are modeled by the Rotne−Prager diffusion tensor[10,24] if the particles do not overlap: for $r_{ij} > \sigma_i + \sigma_j$,

$$\mathbf{D}_{ij} = D_i^0\,\mathbf{I}\delta_{ij} + (1-\delta_{ij})\frac{k_B T}{8\pi\eta r_{ij}^3}\left(\mathbf{I}r_{ij}^2 + \mathbf{r}_{ij}\mathbf{r}_{ij}^T + \frac{\sigma_i^2+\sigma_j^2}{r_{ij}^2}\left(\frac{1}{3}\mathbf{I}r_{ij}^2 - \mathbf{r}_{ij}\mathbf{r}_{ij}^T\right)\right) \quad (8)$$

Here, η is the viscosity of the pure solvent, σ_i is the Stokes radius of the ith particle, δ_{ij} the Kronecker symbol, r_{ij} the distance between particles i and j, and D_i^0 the self-diffusion coefficient of particle i at infinite dilution. This tensor is positive definite by construction (it is strictly an upper bond for the true diffusion tensor); it has, moreover, the property

$$\sum_{j=1}^{N}\frac{\partial}{\partial \mathbf{r}_j}\cdot\mathbf{D}_{ij} = 0 \quad (9)$$

The GS and GC potentials can yield an overlap between particles of different radii, because of their short-range attractive contribution, and we have to evaluate the diffusion tensor even for these configurations. Rotne and Prager[10] gave a mathematical formula for the diffusion tensor of overlapping particles of equal size:

$$\mathbf{D}_{ij} = \frac{k_B T}{6\pi\eta\sigma}\left[\left(1 - \frac{9}{32}\frac{r_{ij}}{\sigma}\right)\mathbf{I} + \frac{3}{32}\frac{\mathbf{r}_{ij}\mathbf{r}_{ij}^T}{\sigma\, r_{ij}}\right] \quad (10)$$

with $\sigma_i = \sigma_j = \sigma$, but there is no expression available at present for overlapping particles of unequal radii. We propose here a simple derivation of the diffusion tensor in the general case of particles of unequal radii, which can overlap.

The Green function method allows to deduce from Stokes equation the velocity field at a distance r_{ij}, due to a force $\mathbf{F}$ acting on a particle i:

$$\eta\mathbf{v} = \left[\beta F(r_{ij})\,\mathbf{I} + \beta G(r_{ij})\frac{\mathbf{r}_{ij}\mathbf{r}_{ij}^T}{r_{ij}^2}\right]\mathbf{F} \quad (11)$$

with

$$\beta F(r) = \Phi(r) - \frac{1}{r^3}\int_0^r dr_1 r_1^2\,\Phi(r_1) \quad (12)$$

$$\beta G(r) = -\Phi(r) + \frac{3}{r^3}\int_0^r dr_1 r_1^2\,\Phi(r_1) \quad (13)$$

where the function Φ is given by

$$\Phi(r) = \frac{1}{4\pi}\frac{1}{\sigma_i} \qquad \text{for} \qquad r \le \sigma_i$$

$$\Phi(r) = \frac{1}{4\pi}\frac{1}{r} \qquad \text{for} \qquad r \ge \sigma_i \quad (14)$$

When particle i is surrounded by other particles with zero size, the mathematical form of the $\mathbf{D}_{ij}$ tensor is easily deduced:

$$\mathbf{D}_{ij} = \frac{1}{\eta}\left[F(r_{ij})\,\mathbf{I} + G(r_{ij})\frac{\mathbf{r}_{ij}\mathbf{r}_{ij}^T}{\mathbf{r}_{ij}^2}\right] \quad (15)$$

For $r_{ij} \ge \sigma_i$, we recover the Rotne−Prager diffusion tensor with $\sigma_j = 0$ and for $r_{ij} \le \sigma_i$ this diffusion tensor is equal to the diffusion coefficient of particle i. This means that particle j with $\sigma_j = 0$ is completely inside particle i and moves with the diffusion coefficient of i. It should be noted that the tensor given by eqs 12, 13, and 15 verifies eq 9. It has been shown by some authors[10,24] that the friction between a particle and the solvent takes place on the spherical surface of the particle rather than at its center. We propose therefore to describe the function Φ by a trial function proportional to the electrostatic interaction between two uniformly charged spherical surfaces rather than by eq 14 and to recalculate the diffusion tensor by using eq 15. This trial function Φ reads as follows: (i) for $r_{ij} \ge \sigma_i + \sigma_j$,

$$\Phi = \frac{1}{4\pi}\frac{1}{r_{ij}} \quad (16)$$

(ii) for $\sigma_j - \sigma_i \le r_{ij} \le \sigma_j + \sigma_i$ with $\sigma_j \ge \sigma_i$,

$$\Phi = \frac{1}{8\pi\sigma_i\sigma_j}\left[\sigma_i + \sigma_j - \frac{r_{ij}}{2} - \frac{(\sigma_j - \sigma_i)^2}{2r_{ij}}\right] \quad (17)$$

(iii) and for $r_{ij} < \sigma_j - \sigma_i$,

$$\Phi = \frac{1}{4\pi}\frac{1}{\sigma_j} \quad (18)$$

By inserting the trial function given by eqs 16, 17, and 18 in eq 15, we finally obtain the following expression for the hydrodynamic diffusion tensor between two spheres of arbitrary radii: (i) for $r_{ij} > \sigma_i + \sigma_j$, we recover the Rotne−Prager diffusion tensor (see eq 8); (ii) for $\sigma_j - \sigma_i \le r_{ij} \le \sigma_i + \sigma_j$, we obtain

$$\mathbf{D}_{ij} = \frac{k_B T}{8\pi\eta\sigma_i\sigma_j}\left[A(r_{ij})\,\mathbf{I} + B(r_{ij})\frac{\mathbf{r}_{ij}\mathbf{r}_{ij}^T}{r_{ij}^2}\right] \quad (19)$$

with

$$A(r) = \frac{2(\sigma_i + \sigma_j)}{3} - \frac{3r}{8} - \frac{(\sigma_j - \sigma_i)^2}{4r} - \frac{(\sigma_j - \sigma_i)^4}{24r^3} \quad (20)$$

$$B(r) = \frac{r}{8} - \frac{(\sigma_j - \sigma_i)^2}{4r} + \frac{(\sigma_j - \sigma_i)^4}{8r^3} \quad (21)$$

If $\sigma_i = \sigma_j$, we recover the formula proposed by Rotne and Prager for overlapping particles of same radii (see eq 10). (iii) for $r_{ij} < \sigma_j - \sigma_i$, we obtain

$$\mathbf{D}_{ij} = \frac{k_B T}{6\pi\eta\sigma_j}\mathbf{I} \quad (22)$$

which means that particle *i* has the same diffusion coefficient as particle *j* if it is completely inside particle *j*.

Rotne and Prager have shown that the diffusion tensor formed by using eq 8 and eq 10 remains positive definite.[10] We have observed in our simulations of $222K^+,Cl^-$ solutions that the diffusion tensor calculated by using eqs 8, 19, and 22 remains positive definite for all situations described here. It should be noticed that the configuration where particle *i* is completely inside particle *j* was hardly ever observed. Although HI are long-ranged, they have been calculated by the latter formulae only for ions included in the cubic simulation box; this approximation has been already discussed in ref 8.

4. Results and Discussion

Figure 1 shows the results of simulations without HI; the computed values obtained with the three interaction potentials presented in section 3 are compared to the experimental data. The results obtained if HI are taken into account are presented in Figure 2.

The comparison between Figures 1 and 2 shows that in all cases, the inclusion of HI in the simulations yields a notable decrease of the equivalent conductance; moreover, the results are in better agreement with experimental data when HI are taken into account. This was already observed in the case of simple electrolytes.[8,9]

The influence of the interaction potential on the computed conductance is strong: the conductance is decreased if the potential contains a short-range attractive contribution (see GS and GC potentials compared to the $1/r^{12}$ potential) and it is decreased especially as the attractive parameter for the + − pair is larger (see the GC potential compared to the GS one). It should be noted that this effect is observed whether HI are taken into account or not. This is in agreement with the usual experimental behavior of the equivalent conductance, which is lowered when ions of opposite charges are associated.

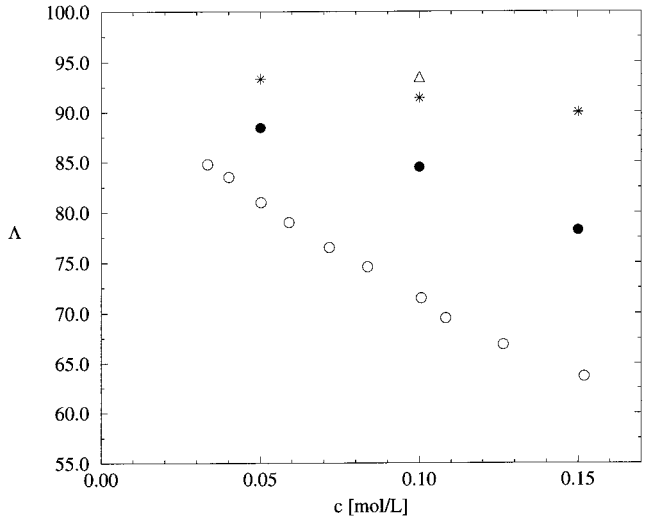

Figure 1. Equivalent conductance [cm^2/mol/Ω] of aqueous $222K^+,Cl^-$ solutions at 298 K obtained from simulations without HI: (○) experiments, (★) GS potential, (△) $1/r^{12}$ potential, and (●) GC potential.

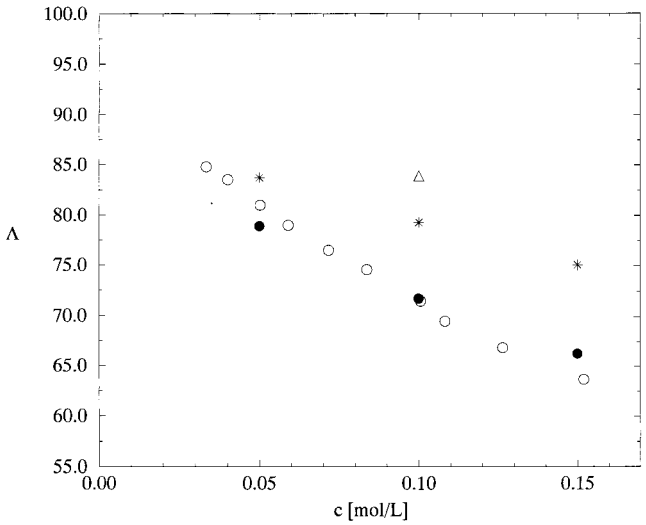

Figure 2. Equivalent conductance [cm^2/mol/Ω] of aqueous $222K^+,Cl^-$ solutions at 298 K obtained from simulations with HI: (○) experiments, (★) GS potential, (△) $1/r^{12}$ potential, and (●) GC potential.

The simulation results are in good agreement with experimental data when interactions between ions are modelled by the GC potential, i.e., by a potential which contains an intensive short-range attractive contribution for the + − pair in addition to the Coulomb and repulsive potentials. The GS potential which was fitted to SANS experiments enabled to interpret some of the properties of the solution at 0.5 mol/L but seems to underestimate the attraction between the ions.

The pair correlation functions obtained from the GS and GC potentials are given in Figure 3; the increase of the short-range attraction for the + − pair (see GC potential compared to the GS one) leads to an increase of the intensities of all pair correlation functions. On the other hand, it should be noted that the position of the peak of $g_{+-}(r)$ does not change when the A_{+-} parameter is varied. This means that the GC potential leads to a stronger association between cation and anion than the GS one, without changing the spatial structure of this association.

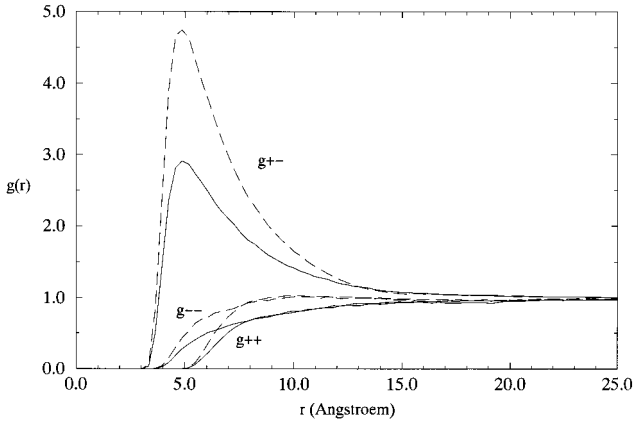

Figure 3. Ion pair correlation functions obtained from BD simulations for a 0.1 mol/L aqueous solution of $222K^+$,Cl^- at 298K: (—) GS potential, (− −) GC potential.

As the computed conductance is decreased when the attraction for the + − pair is increased, one could suggest that a stronger attraction could lead to a better agreement with experimental results *even if* HI are not taken into account. We have therefore performed numerical simulations with an interaction potential similar to the GS and GC ones, now with $A_{+-} = -150$ J/mol, but we observed that this strong attraction leads to unphysical results (aggregation of the particles). This implies that even for an associated electrolyte, HI must be taken into account to describe the dynamical properties of the solution.

The last point we have to discuss concerns the difficulty for the system studied here to find an interaction potential which describes both structural and dynamical properties: the potential GS which gives the SANS spectrum at 0.5 mol/L does not give the conductance below 0.15 mol/L and the potential GC which gives the conductance below 0.15 mol/L will not allow to describe the SANS spectrum at 0.5 mol/L, because the pair correlation functions obtained at 0.1 mol/L from the GS and GC potentials are different (see Figure 3). A fit of the potential parameters simultaneously to SANS and to a dynamical property should be done at a same concentration, as in ref 25. In our case, the simulation of more concentrated cryptate chloride solutions should not be performed by the method presented in section 2 as the approximation of pairwise additivity of HI is reasonable only for systems of relatively low packing fraction;[26] on the other hand relevant SANS experiments cannot be obtained for dilute solutions.

Finally, it should be pointed out that the difference between experiments and simulation results with the GS potential in the case with HI could be partially due to our approximated treatment of HI in the case of overlapping particles (see section 2).

5. Conclusion

In the present work, we have computed the electrical conductance of aqueous cryptated potassium chloride solutions below 0.15 mol/L. The interaction potential used in these simulations contains a strong short-range attractive contribution which can yield an overlap between ions. We have therefore proposed an approximate expression of the hydrodynamic diffusion tensor for particles of arbitrary radii which can overlap. As in the case of simple electrolytes,[8,9] it has been observed that the inclusion of HI leads to a systematic decrease of the equivalent conductance.

The potential proposed by Cartailler et al.[6] to interpret the SANS experiments at 0.5 mol/L, which give information on the structural properties of the solution, does not yield dynamical simulation results in good agreement with experimental data at concentrations below 0.15 mol/L. An enhancement of the short-range attractive parameter for the + − pair allowed to obtain conductivities closer to our experimental results.

For the system studied here, we have shown that it is difficult to propose an interaction potential which describes both structural and dynamical properties of the solution, for a large range of concentrations. It would be interesting to study other structural or dynamical properties of these solutions (e.g., osmotic pressure, activity coefficients or self-diffusion coefficients, etc.) in order to refine the interaction model; on the other hand, the treatment of HI should be improved in the case of associated electrolytes.

Acknowledgment. We gratefully acknowledge T. Cartailler for helpful discussion and comments.

References and Notes

(1) Lehn, J.-M. *J. Inclusion Phenom.* **1988**, *6*, 351.
(2) Kauffmann, E.; Lehn, J.-M.; Sauvage, J.-P. *Helv. Chim. Acta* **1976**, *59*, 1099.
(3) D'Aprano, A.; Sesta, B. *J. Sol. Chem.* **1988**, *17*, 117.
(4) Buschmann, H.-J. *Inorg. Chim. Acta* **1992**, *195*, 51.
(5) Kunz, W.; Calmettes, P.; Turq, P.; Cartailler, T.; Morel-Desrosiers, N.; Morel, J.-P. *J. Chem. Phys.* **1992**, *97*, 5647.
(6) Cartailler, T.; Calmettes, P.; Kunz, W.; Turq, P.; Rossy-Delluc, S. *Mol. Phys.* **1993**, *80*, 833.
(7) Rossky, P. J.; Doll, J. D.; Friedman, H. L. *J. Chem. Phys.* **1978**, *69*, 4628.
(8) Jardat, M.; Bernard, O.; Turq, P.; Kneller, G. R. *J. Chem. Phys.* **1999**, *110*, 7993.
(9) Jardat, M.; Durand-Vidal, S.; Turq, P.; Kneller, G. R. *J. Mol. Liq.* **1999**. In press.
(10) Rotne, J.; Prager, S. *J. Chem. Phys.* **1969**, *50*, 4831.
(11) Lind, J. F., Jr.; Zwolenik, J. J.; Fuoss, R. M. *J. Am. Chem. Soc.* **1959**, *81*, 1557.
(12) Barthel, J.; Feuerlein, F.; Neueder, R.; Wachter, R. *J. Sol. Chem.* **1980**, *9*, 209.
(13) Ermak, D. L. *J. Chem. Phys.* **1975**, *62*, 4189.
(14) Van Kampen, N. G. *Stochastic Processes in Physics and Chemistry*; North-Holland Personal Library: New York, 1987.
(15) Felderhof, B. U.; Jones, R. B. *Phys. A* **1983**, *119*, 591.
(16) Ramanathan, P. S.; Friedman, H. L. *J. Chem. Phys.* **1971**, *54*, 1086.
(17) Allen, M. P.; Tildesley, D. J. *Computer Simulation of Liquids*; Oxford Science Publications: Oxford, 1987.
(18) de Leeuw, S. W.; Perram, J. W.; Smith, E. R. *Proc. R. Soc. London* **1980**, *A 373*, 27.
(19) Kneller, G. R.; Keiner, V.; Kneller, M.; Schiller, M. *Comput. Phys. Commun.* **1995**, *91*, 191.
(20) Rossy-Delluc, S.; Cartailler, T.; Tivant, P.; Turq, P.; Morel-Desrosiers, N. *Mol. Phys.* **1994**, *82*, 701.
(21) Rossy-Delluc, S.; Cartailler, T.; Turq, P.; Bernard, O.; Morel-Desrosiers, N.; Morel, J.-P.; Kunz, W. *J. Phys. Chem.* **1993**, *97*, 5136.
(22) Lehmani, A.; Cartailler, T.; Rossy-Delluc, S.; Turq, P. *J. Electroanal. Chem.* **1996**, *416*, 121.
(23) Robinson, R. A.; Stokes, R. H. *Electrolyte Solutions*. Butterworths: Markham, ON, 1959.
(24) Garcia de la Torre, J.; Bloomfield, V. A. *Quat. Rev. Biophys.* **1981**, *14*, 81.
(25) Kunz, W.; Turq, P.; Bellissent-Funel, M.-C.; Calmettes, P. *J. Chem. Phys.* **1991**, *95*, 6902.
(26) Beenakker, C. W. J.; Mazur, P. *Phys. A* **1983**, *120*, 388.